Smart Structures and Systems, *Vol. 17, No. 5 (2016) 753-771*
DOI: http://dx.doi.org/10.12989/sss.2016.17.5.753

Free and transient responses of linear complex stiffness system by Hilbert transform and convolution integral

S.H. Bae[1], J.R. Cho[*2] and W.B. Jeong[1]

[1]*School of Mechanical Engineering, Pusan National University, Busan 609-735, Korea*
[2]*Department of Naval Architecture and Ocean Engineering, Hongik University, Sejong 339-701, Korea*

(Received April 14, 2015, Revised February 7, 2016, Accepted February 14, 2016)

Abstract. This paper addresses the free and transient responses of a SDOF linear complex stiffness system by making use of the Hilbert transform and the convolution integral. Because the second-order differential equation of motion having the complex stiffness give rise to the conjugate complex eigen values, its time-domain analysis using the standard time integration scheme suffers from the numerical instability and divergence. In order to overcome this problem, the transient response of the linear complex stiffness system is obtained by the convolution integral of a green function which corresponds to the unit-impulse free vibration response of the complex system. The damped free vibration of the complex system is theoretically derived by making use of the state-space formulation and the Hilbert transform. The convolution integral is implemented by piecewise-linearly interpolating the external force and by superimposing the transient responses of discretized piecewise impulse forces. The numerical experiments are carried out to verify the proposed time-domain analysis method, and the correlation between the real and imaginary parts in the free and transient responses is also investigated.

Keywords: linear complex stiffness system; free and transient responses; time domain analysis; Hilbert transform; state-space formulation; convolution integral

1. Introduction

Viscoelastic materials such as elastomer are widely used in various engineering applications to reduce the structural vibration and noise, to protect the interior contents from the outside, to maintain the ground traction force, and so on. For example, in the structural vibration field, rubber mounts are used to isolate the structural system from the external excitation and the damped sandwich beams in which rubber layers are inserted between metallic layers absorb the structural vibration energy via the hysteretic loss of the rubber layers (Mead and Markus 1969, Sainsbury and Masti 2007, Mohammandi and Sedaghati 2012, Hajianmaleki and Qatu 2013, Won *et al*. 2013). These damped structures are not so difficult to manufacture by current manufacturing technology, but, differing from the elastic structures, their mathematic analysis still remains as an important research subject owing to the existence of damping (Crandall 1995, Chen and You 1997, Genta and Amati 2010, Cho *et al*. 2012, Zhu *et al*. 2014). There have been introduced various

∗Corresponding author, Associate Professor, E-mail: jrcho@hongik.ac.kr

http://www.techno-press.org/?journal=sss&subpage=8 ISSN: 1738-1584 (Print), 1738-1991 (Online)

mathematic models to express the damping characteristics of viscoelastic materials, among which the hysteretic damping model (Meirovitch 1986, Chen *et al*. 1994) is widely used to express the complex stiffness. A complex number gives rise to the phase difference in the frequency response which causes the energy dissipation, so that the characteristic of complex stiffness is consistent well with the hysteretic damping.

Meanwhile, most of previous theoretical and numerical studies on the complex stiffness systems were made in the frequency domain, in which the external excitation is expressed as harmonic force so that the imaginary part is automatically defined. However, in case of the time-domain analysis, the external force is real contrary to the complex-valued equations of motion. What is worse, a state-space formulation of complex stiffness system for obtaining the complex time response leads to two poles in the radial symmetry in the complex plane (Inaudi and Makris 1996). One pole is stable but the other pole having a positive real eigen value is unstable such that the time response obtained by the standard time integration techniques suffers from the unbounded growth with the lapse of time. In order to obtain the consistent time-domain formulation and the stable bounded time response, Inaudi and Markis (1996) used the Hilbert transform and the inverse Fourier transform (IFT) and employed the time reversal technique (Fink 1992). Salehi *et al*. (2008) applied the inverse Fourier transform (IFT) to solve the time response of damped sandwich structures. But, the Hilbert transform of external excitation using the discrete Fourier transform and inverse Fourier transform (IFT) may produce the imaginary force signal that is different from the analytically derived exact one, because the external excitation is considered as a periodic function in the course of Fourier transform. This periodicity assumption of external force strongly affects the time response, which results in the incorrect time response of complex stiffness system (Bae *et al*. 2014a).

In the time reversal technique (Nguyen *et al*. 2005, Padois *et al*. 2012, Li *et al*. 2012), where the time differential equation corresponding to the unstable pole is converted to one running backwards in time, the initial conditions of the system at the negative infinity are assumed to be clearly identified. In acoustic and medical applications where the time responses are obtained based on the outdoor measurements, the identification of initial conditions at negative infinity is not difficulty but straightforward. But, it becomes a highly difficult and troublesome task in case of the complex stiffness system which is not relied on measurements. In our previous work aiming at the development of a reliable time-domain analysis method for five-layered damped sandwich beams (Bae *et al*. 2014a, b), a discrete convolutional Hilbert transform using the consistent imaginary initial conditions and its time-duration extended superposition scheme have been introduced to overcome the above-mentioned problems. Where, the focus was made only on the free response-dominated vibration behavior of damped beam structures by applying the impulse loading.

In other words, whether the transient response to the non-impulse force could be successfully obtained or not and the characteristic difference between the free and transient responses obtained by the proposed method still remains in doubt. In this context, this paper extends our previous work to the transient response of linear dynamic problem having the complex stiffness, in order to investigate the above-mentioned subject using a less complicated single-degree-of-freedom (SDOF) problem. In particular, the correlation between the real and imaginary parts in the free and transient responses, its useful usage, and the limitation of the proposed time-domain analysis method are examined. The free response of the complex system which is divided into the real and imaginary parts, where the imaginary part is assumed to be the Hilbert transform of the real part, is theoretically derived in the state-space formulation by considering the initial conditions and by

excluding the positive real eigen values. An arbitrary non-impulse force is divided into piecewise linear impulses and the transient response of complex dynamic system is numerically obtained by superimposing the piecewise transient responses. Here, The piecewise transient responses are calculated by the convolution integral of the piecewise impulse and the unit impulse response which is derived by applying the unit initial velocity to the system free response.

As an extension of our previous work (Bae *et al.* 2014a, c), we in this paper intends to investigate in depth the above-mentioned characteristics of the free and transient responses of complex stiffness SDOF system that are obtained by the Hilbert transform and convolution integral. This paper is organized as follows. The relation between the Hilbert transform and the Fourier transform (FT) and the equation of motion of a SDOF linear dynamic system having the complex stiffness are introduced in Section 2. Next, the theoretical derivation of the free response of complex stiffness system in the state-space formulation by utilizing the Hilbert transform is described in Section 3. The convolution integral of the unit-impulse free response and its numerical implementation for obtaining the complex transient response are explained in Section 4. The numerical experiments illustrating the proposed method, together with the investigation on the correlation between the real and imaginary parts in the free and transient responses, are presented in Section 5, and the conclusion is made in Section 6.

2. Hilbert transform and a SDOF linear complex stiffness system

The Hilbert transform $\mathrm{H}[f(t)]$ of a signal $f(t)$ is a phase-shifting but magnitude-conserving linear operator (Johansson 1999, Luo *et al.* 2009, Wang *et al.* 2015) defined by the convolution of $f(t)$ such that

$$\hat{f}(t)=\mathrm{H}[f(t)]=\frac{1}{\pi}\lim_{a\to\infty}\mathrm{P}\int_{-a}^{a}\frac{f(\tau)}{t-\tau}d\tau \tag{1}$$

with P being the Cauchy principal value given by

$$\mathrm{P}\int_{-a}^{a}\frac{f(\tau)}{t-\tau}d\tau=\lim_{\varepsilon\to 0^{+}}\left[\int_{-a}^{t-\varepsilon}\frac{f(\tau)}{t-\tau}d\tau+\int_{t+\varepsilon}^{a}\frac{f(\tau)}{t-\tau}d\tau\right] \tag{2}$$

Since the Hilbert transform is defined by the convolution: $\hat{f}(t)=f(t)*(1/\pi t)$ and the Fourier transform (FT) of $(1/\pi t)$ becomes

$$\mathrm{FT}\left[1/\pi t\right]=-\mathrm{j}\,\mathrm{sgn}(\omega) \tag{3}$$

with $\mathrm{sgn}(\omega)=-1$ for $\omega<0$, 0 for $\omega=0$ and 1 for $\omega>0$, the Fourier transform $\hat{F}(\omega)$ of the Hilbert transform $\hat{f}(t)$ can be obtained using the Fourier transform $F(\omega)$ of the original signal $f(t)$ such that

$$\mathrm{FT}\left[\hat{f}(t)\right]=\hat{F}(\omega)=-\mathrm{j}\,\mathrm{sgn}(\omega)F(\omega) \tag{4}$$

Thus, the Fourier transform of a strong analytic signal $f_a(t)=f(t)+\mathrm{j}\,\hat{f}(t)$ which is composed of the real and imaginary parts becomes

$$\mathrm{FT}\left[f_a(t)\right] = F_a(\omega) = F(\omega) + \mathrm{sgn}(\omega)F(\omega) \tag{5}$$

Furthermore, from the relation given in Eq. (4), the strong analytic signal $f_a(t) = f(t) + \mathrm{j}\hat{f}(t)$ can be obtained by the inverse Fourier transform (IFT) of the one-side-spectrum $F^+(\omega)\left(= F(\omega), \omega > 0\right)$:

$$\mathrm{IFT}\left[2F^+(\omega)\right] = f_a(t) \tag{6}$$

In this manner, the analytic signal of the real applied load for the time-domain analysis of linear complex stiffness system could be obtained by a combined use of FT and IFT.

The equations of motion for the complex dynamic system are usually expressed in the frequency domain, so that we convert the form into the time domain using the inverse Fourier transform and the Hilbert transform. The equation of motion in the frequency domain for a SDOF linear complex stiffness system having the loss factor η is expressed by

$$-\omega^2 mX(\omega) + \left(k + \mathrm{j}\, k\eta\, \mathrm{sgn}(\omega)\right)X(\omega) = F(\omega) \tag{7}$$

with $X(\omega)$ being the frequency response function. Using the relation (4), it can be rewritten as

$$-\omega^2 mX(\omega) + kX(\omega) - k\eta\hat{X}(\omega) = F(\omega) \tag{8}$$

and taking the Hilbert transform leads to

$$-\omega^2 m\hat{X}(\omega) + k\hat{X}(\omega) + k\eta X(\omega) = \hat{F}(\omega) \tag{9}$$

Multiplying j to Eq. (9) and combining Eqs. (8) and (9), one can obtain the equation of motion in the frequency domain given by

$$-\omega^2 mX_a(\omega) + kX_a(\omega) + \mathrm{j}k\eta X_a(\omega) = F_a(\omega) \tag{10}$$

in the form of Fourier transform of analytic functions. Then, by taking the inverse Fourier transform, one can derive the equation of motion in the time domain given by

$$m\ddot{x}_a(t) + k(1 + \mathrm{j}\,\eta)x_a(t) = f_a(t) \tag{11}$$

to obtain the complex time response $x_a(t)$ of a SDOF linear complex stiffness system.

3. State-space formulation for the free vibration response

In this section, the free response of a SDOF problem in Eq. (11) in the time domain is derived according to the state-space formulation. Differing from the time reversal technique in which the initial conditions at the negative infinity (i.e., at $t = -\infty$) should be specified, this approach allows one to derive the consistent imaginary initial conditions at $t = 0$. Furthermore, the unstable pole causing the unbounded growth in the time response could be excluded in the course of derivation. By letting $x_a(t)$ be $u(t) + \mathrm{j}v(t)$, the free vibration problem (11) is split into two ordinary differential equations given by

$$m\ddot{u}(t)+ku(t)-k\eta v(t)=0 \tag{12}$$

$$m\ddot{v}(t)+k\eta u(t)+kv(t)=0 \tag{13}$$

with the prescribed initial conditions $u(0)=u_0$ and $\dot{u}(0)=\dot{u}_0$.

Here, it is assumed that $v(t)=H[u(t)]$ be a Hilbert transform of $u(t)$ by letting $x_a(t)=u(t)+\mathrm{j}v(t)$. One can solve Eq. (11) by deriving the analytic external force $f_a(t)$ and by employing the time-reversal technique to obtain two stable differential equations which are expressed in terms of the analytic modal coordinates $q_1(t)$ and $q_2(t)$, as represented in (Inaudi and Makris 1996). However, we in this study let $v(t)=H[u(t)]$ to derive the consistent imaginary initial conditions $v(0)$ and $\dot{v}(0)$ through the state-space formulation, and to get $v(t)$ that is expected to satisfy $H[u(t)]$ by specifying the derived imaginary initial conditions, as represented in our previous paper in detail (Bae *et al.* 2014a). These two differential equations are not completely separated but correlated via the phase shift, so those are rewritten in the following matrix defined by

$$\frac{d}{dt}\begin{Bmatrix} u \\ \dot{u} \\ v \\ \dot{v} \end{Bmatrix}=\begin{bmatrix} 0 & 1 & 0 & 0 \\ -\omega_n^2 & 0 & \eta\omega_n^2 & 0 \\ 0 & 0 & 0 & 1 \\ -\eta\omega_n^2 & 0 & \omega_n^2 & 0 \end{bmatrix}\begin{Bmatrix} u \\ \dot{u} \\ v \\ \dot{v} \end{Bmatrix} \tag{14}$$

according to the state-space formulation. For the sake of concise expression, it is further written in a simple form given by

$$\{\dot{\mathbf{x}}_a\}=[\mathbf{L}]\{\mathbf{x}_a\} \tag{15}$$

In the mode coordinates, a general solution $\mathbf{x}_a(t)=\{u,\dot{u},v,\dot{v}\}^T$ is expanded in terms of the matrix $[\mathbf{V}]$ of complex mode vectors and the analytic modal coordinates $\{\mathbf{p}\}$ as

$$\{\mathbf{x}_a\}=[\mathbf{V}]\{\mathbf{p}\} \tag{16}$$

Substituting Eq. (16) into Eq. (15) ends up with the complex eigen-value problem given by

$$\{\dot{\mathbf{p}}\}=[\mathbf{V}]^{-1}[\mathbf{L}][\mathbf{V}]\{\mathbf{p}\}=[\lambda]\{\mathbf{p}\} \tag{17}$$

For the SDOF linear complex stiffness system in Eq. (11), the matrix of complex eigen values is defined by

$$[\lambda]=\begin{bmatrix} z & 0 & 0 & 0 \\ 0 & \bar{z} & 0 & 0 \\ 0 & 0 & -\bar{z} & 0 \\ 0 & 0 & 0 & -z \end{bmatrix} \tag{18}$$

with $z=\omega_n\sqrt{-1+\mathrm{j}\eta}=\alpha_R+\mathrm{j}\alpha_I$. Here, the real and imaginary parts of the complex eigen values are defined by $\alpha_R^2=\left(\sqrt{1+\eta^2}-1\right)\omega_n^2/2$ and $\alpha_I^2=\left(\sqrt{1+\eta^2}+1\right)\omega_n^2/2$ respectively. And, by letting $\sqrt{2+2s}$ be r with $s=\alpha_R^2+\alpha_I^2$, the matrix $[\mathbf{V}]$ is expressed by four complex column mode vectors $\mathbf{V_i}$ as follows

$$[\mathbf{V}]=[\mathbf{V}_1,\mathbf{V}_2,\mathbf{V}_3,\mathbf{V}_4]=\frac{1}{r}\begin{bmatrix}-\mathrm{j}/z & \mathrm{j}/\bar{z} & -\mathrm{j}/\bar{z} & \mathrm{j}/z\\ -\mathrm{j} & \mathrm{j} & \mathrm{j} & -\mathrm{j}\\ 1/z & 1/\bar{z} & -1/\bar{z} & -1/z\\ 1 & 1 & 1 & 1\end{bmatrix} \tag{19}$$

Then, referring to our previous work (Bae *et al*. 2014a), the general solution $\boldsymbol{x}_a(t)=\{u,\dot{u},v,\dot{v}\}^T$ in Eq. (16) is expressed by

$$\mathbf{x}_a(t)=c_1\mathrm{e}^{zt}\mathbf{X}_1^*+\bar{c}_1\mathrm{e}^{\bar{z}t}\mathbf{X}_2^*+c_2\mathrm{e}^{-\bar{z}t}\mathbf{X}_3^*+\bar{c}_2\mathrm{e}^{-zt}\mathbf{X}_4^* \tag{20}$$

with complex constants $c_1=a_1+\mathrm{j}b_1$, $c_2=a_2+\mathrm{j}b_2$ and their conjugates $\bar{c}_1$ and $\bar{c}_2$. Here, four complex eigen vectors $\mathbf{X}_1^*,\mathbf{X}_2^*,\mathbf{X}_3^*,\mathbf{X}_4^*$ are defined by $\mathbf{X}_{1,2}^*=\mathbf{V}_1\pm j\mathbf{V}_2$ and $\mathbf{X}_{3,4}^*=\mathbf{V}_3\pm j\mathbf{V}_4$. By expanding Eq. (20), it is not hard to obtain a complex-valued vector equation given by

$$\mathbf{x}_a(t)=2\mathrm{Re}\left[c_1\mathrm{e}^{zt}\left(\mathbf{V}_1+\mathrm{j}\mathbf{V}_2\right)\right]+2\mathrm{Re}\left[c_2\mathrm{e}^{-\bar{z}t}\left(\mathbf{V}_3+\mathrm{j}\mathbf{V}_4\right)\right] \tag{21}$$

Letting $A=2a_1, B=-2b_1, C=2a_2$ and $D=-2b_2$, Eq. (21) ends up with a real-valued sinusoidal function

$$\begin{aligned}\mathbf{x}_a(t)=\mathrm{e}^{\alpha_R t}&\left[\left(A\cos(\alpha_I t)+B\sin(\alpha_I t)\right)\mathrm{Re}\mathbf{V}_1+\left(B\cos(\alpha_I t)-A\sin(\alpha_I t)\right)\mathrm{Im}\mathbf{V}_1\right]\\ +\mathrm{e}^{-\alpha_R t}&\left[\left(C\cos(\alpha_I t)+C\sin(\alpha_I t)\right)\mathrm{Re}\mathbf{V}_1+\left(D\cos(\alpha_I t)-C\sin(\alpha_I t)\right)\mathrm{Im}\mathbf{V}_1\right]\end{aligned} \tag{22}$$

Two constants A and B should vanish because $\boldsymbol{x}(t)$ vanishes as t goes to infinity, and the following coupled equation system for determining the imaginary initial conditions for $v(t)$ is obtained

$$\mathbf{x}_a(0)=\begin{Bmatrix}u_0\\ \dot{u}_0\\ v_0\\ \dot{v}_0\end{Bmatrix}=\frac{1}{r}\begin{bmatrix}\alpha_I/s & -\alpha_R/s\\ 0 & 1\\ -\alpha_R/s & -\alpha_I/s\\ 1 & 0\end{bmatrix}\begin{Bmatrix}C\\ D\end{Bmatrix} \tag{23}$$

Using the given initial conditions y_0 and $\dot{y}_0$ of the real part $u(t)$, one can get two constants: $C=\left(su_0+\alpha_R\dot{u}_0\right)r/\alpha_I$ and $D=r\dot{u}_0$ and the imaginary initial conditions given by

$$v_0 = -\frac{\dot{u}_0 + \alpha_R u_0}{\alpha_I}, \quad \dot{v}_0 = \frac{\alpha_R \dot{u}_0 + s u_0}{\alpha_I} \tag{24}$$

By substituting these four constants into Eqs. (19) and (22), one can get the complex free response given by

$$\begin{Bmatrix} u(t) \\ v(t) \\ \dot{u}(t) \\ \dot{v}(t) \end{Bmatrix} = \mathrm{e}^{-\alpha_R t} \begin{bmatrix} \cos(\alpha_I t) & -\sin(\alpha_I t) & 0 & 0 \\ \sin(\alpha_I t) & \cos(\alpha_I t) & 0 & 0 \\ 0 & 0 & \cos(\alpha_I t) & -\sin(\alpha_I t) \\ 0 & 0 & \sin(\alpha_I t) & \cos(\alpha_I t) \end{bmatrix} \begin{Bmatrix} u_0 \\ v_0 \\ \dot{u}_0 \\ \dot{v}_0 \end{Bmatrix} \tag{25}$$

This form of solution justifies our assumption that $x_a(t) = u(t) + \mathrm{j}v(t)$ is related to the Hilbert transform. In order words, $u(t)$ and $\dot{u}(t)$ are expressed by a product of the low- and high-pass signals with non-overlapping spectra, and their Hilbert transforms $v(t)$ and $\dot{v}(t)$ are defined by a product of the low-pass signal and the Hilbert transform of high-pass signal. And, the Fourier transforms of these functions are defined over the upper half-plane $[0, +\infty)$ in accordance with the problem definition in Eq. (7).

4. Convolution integral for the transient time response

The transient time response $\mathbf{x}_a(t) = \{u(t), \dot{u}(t), v(t), \dot{v}(t)\}^T$ of a SDOF complex stiffness system subject to the external excitation $f(t)$ is obtained by the convolution integral given by

$$\mathbf{x}_a(t) = \int_0^t f(\tau)\mathbf{g}(t-\tau)d\tau \tag{26}$$

where $\mathbf{g}(t) = \{u(t), \dot{u}(t), v(t), \dot{v}(t)\}^T$ indicates the unit impulse response of the complex stiffness system. The unit impulse response $\mathbf{g}(t)$ can be obtained from Eq. (25) using $u_0 = 0, \dot{u}_0 = 1/m$, $v_0 = -1/m\alpha_I$ and $\dot{v}_0 = \alpha_R / m\alpha_I$ (Rao 1995), where m indicates the mass of the dynamic system. The analytic convolution integral (26) is numerically implemented by three different methods in the current study, the superposition method and the zero- and first-order approximation methods. For the numerical convolution integral, a continuous external force $f(t)$ is firstly approximated by a discrete one $Df(t)$ as shown in Fig. 1, where the divided discrete forces are either piecewise constant or piecewise linear.

In the superposition method, individual piecewise constant forces are considered as an impulse force with the magnitude of $f_k \Delta t = f(t_k)\Delta t$ and their contributions to the entire transient response are superimposed as following

$$\mathbf{x}_a(t) = \sum_{k=1}^{n-1} f_k \, \mathbf{g}(t - t_k)\Delta t, \quad f_k = f(t_k) \tag{27}$$

Eq. (27) is nothing but a numerical integration form (Rao 1995) of the mathematical

convolution integral (26). The zero-order approximation method does also use the piecewise constant impulse forces like the superposition method, but the convolution integral is differently implemented based on the time-incremental approach. In other words, the transient response $\mathbf{x}_{k+1}$ at the next time step is obtained by adding the additional convolution integral of the discrete impulse force f_{k+1} applied during the time interval Δt to the free response given in Eq. (25) at the current time step. This approach is based on the fact that the solution of a linear second-order differential equation is composed of the homogeneous free response and the particular solution to the external force. For the sake of convenience, let us introduce two functions $\mathrm{esi}(\Delta t)$ and $\mathrm{eco}(\Delta t)$ defined by

$$\mathrm{esi}(\Delta t)=\int_0^{\Delta t} \mathrm{e}^{-\alpha_r(t-\tau)}\sin(\alpha_I(t-\tau))d\tau,\quad \mathrm{eco}(\Delta t)=\int_0^{\Delta t} \mathrm{e}^{-\alpha_r(t-\tau)}\cos(\alpha_I(t-\tau))d\tau \tag{28}$$

Then, the transient response $\boldsymbol{x}_{k+1}=\{u_{k+1},\dot{u}_{k+1},v_{k+1},\dot{v}_{k+1}\}^T$ at the next time step t_{k+1} is calculated using the iterative incremental form given by

$$\begin{Bmatrix} u \\ v \\ \dot{u} \\ \dot{v} \end{Bmatrix}_{k+1} = f_{k+1}\begin{Bmatrix} ED_u(\Delta t) \\ ED_v(\Delta t) \\ EV_u(\Delta t) \\ EV_v(\Delta t) \end{Bmatrix} + \mathrm{e}^{-\alpha_R \Delta t}\begin{bmatrix} \cos(\alpha_I\Delta t) & -\sin(\alpha_I\Delta t) & 0 & 0 \\ \sin(\alpha_I\Delta t) & \cos(\alpha_I t) & 0 & 0 \\ 0 & 0 & \cos(\alpha_I t) & -\sin(\alpha_I t) \\ 0 & 0 & \sin(\alpha_I\Delta t) & \cos(\alpha_I\Delta t) \end{bmatrix}\begin{Bmatrix} u \\ v \\ \dot{u} \\ \dot{v} \end{Bmatrix}_k \tag{29}$$

with $ED_u(\Delta t)=\mathrm{esi}(\Delta t)/m\alpha_I$, $ED_v(\Delta t)=-\mathrm{eco}(\Delta t)/m\alpha_I$, $EV_u(\Delta t)=\mathrm{eco}(\Delta t)/m-\alpha_R\mathrm{esi}(\Delta t)/m\alpha_I$ and $EV_v(\Delta t)=\mathrm{esi}(\Delta t)/m+\alpha_R\mathrm{eco}(\Delta t)/m\alpha_I$. The first term at the RHS of Eq. (29) indicates the additional convolution integral due to the discrete impulse force f_{k+1} while the second term is the free response increment.

Meanwhile, in the first-order approximation, the discrete impulse force f_{k+1} at time state t_{k+1} consists of f_k and the linear increment $\Delta f_k = f_{k+1} - f_k$ as represented in Fig. 1. Thus, the force increment Δf_k gives rise to the additional contribution to the convolution integral of the zero-order approximation. By introducing two additional exponential harmonic functions defined by

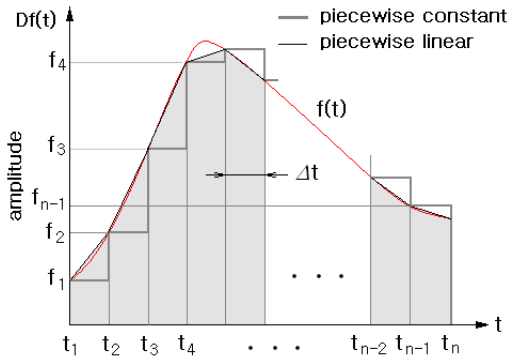

Fig. 1 Discretization of a continuous signal into a finite number of discrete impulses

$$\text{lesi}(\Delta t)=\int_0^{\Delta t} \tau\, \mathrm{e}^{-\alpha_r(t-\tau)}\sin(\alpha_I(t-\tau))d\tau,\quad \text{leco}(\Delta t)=\int_0^{\Delta t} \tau\, \mathrm{e}^{-\alpha_r(t-\tau)}\cos(\alpha_I(t-\tau))d\tau \tag{30}$$

to compute the additional convolution contribution by the force increment Δf_k, the iterative incremental form (29) is modified as follows

$$\begin{Bmatrix} u \\ v \\ \dot{u} \\ \dot{v} \end{Bmatrix}_{k+1} = \Delta f_k \begin{Bmatrix} LED_u(\Delta t) \\ LED_v(\Delta t) \\ LEV_u(\Delta t) \\ LEV_v(\Delta t) \end{Bmatrix} + f_k \begin{Bmatrix} ED_u(\Delta t) \\ ED_v(\Delta t) \\ EV_u(\Delta t) \\ EV_v(\Delta t) \end{Bmatrix} + FRI_k \tag{31}$$

where, FRI_k indicates the free response increment (i.e., the second term at the RHS of Eq. (29)), and the new quantities are defined by $LED_u(\Delta t)=\text{lesi}(\Delta t)/m\alpha_I\Delta t, LED_v(\Delta t)=-\text{leco}(\Delta t)/m\alpha_I\Delta t$, $LEV_u(\Delta t)=\text{leco}(\Delta t)/m\Delta t-\alpha_R\text{lesi}(\Delta t)/m\alpha_I\Delta t$ and $LEV_v(\Delta t)=\text{lesi}(\Delta t)/m\Delta t+\alpha_R\text{leco}(\Delta t)/m\alpha_I\Delta t$ respectively.

5. Numerical results

In order to illustrate the fact that the solution $\boldsymbol{x}_a(t)$ given in Eq. (25) is related to the Hilbert transform, we revisit a SDOF complex stiffness system (Bae *et al.* 2014c) given by

$$\ddot{x}_a(t)+(50)^2(1+0.2\,\mathrm{j})x_a(t)=0 \tag{32}$$

with the predefined initial conditions: $u(0)=0$ and $\dot{u}(0)=1$. The real and imaginary parts of the dynamic displacement and velocity are represented in Fig. 2. It is observed that each component is exponentially decaying at the beginning and then the sinusoidal free response, that is, a product of the low- and high-pass signals. Further, it is found from the comparison between the real and imaginary parts that the phases are shifted by $\pi/2$ but the magnitudes are conserved.

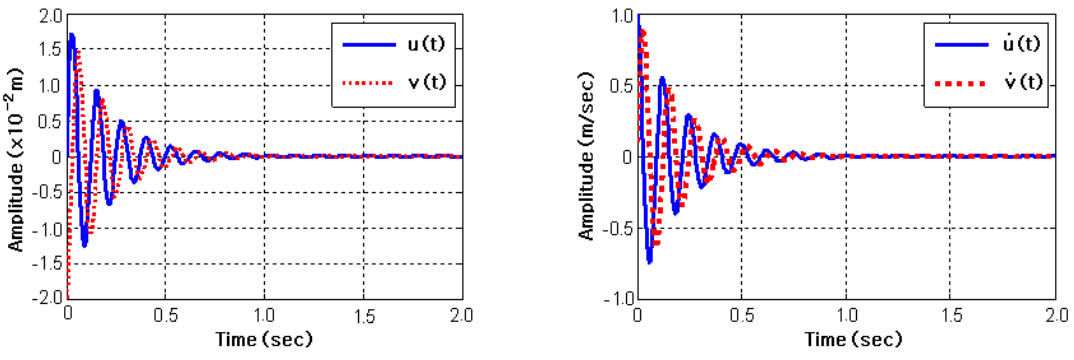

(a) (b)

Fig. 2 Free vibration response of the problem (Bae *et al.* 2014c): (a) displacement and (b) velocity

A trajectory of $u(t)$ and $v(t)$ on the complex plane is shown in Fig. 3, where the solution characteristic of a SDOF complex stiffness system is well observed. The complex displacement $u(t)+jv(t)$ is characterized by the exponentially decaying behavior and the rotation behavior, which is consistent with the fact that the complex solution is expressed by

$$\begin{Bmatrix} u(t) \\ v(t) \end{Bmatrix} = \mathrm{e}^{-\alpha_R t} \begin{bmatrix} \cos(\alpha_I t) & -\sin(\alpha_I t) \\ \sin(\alpha_I t) & \cos(\alpha_I t) \end{bmatrix} \begin{Bmatrix} u_0 \\ v_0 \end{Bmatrix} = \mathrm{e}^{-\alpha_R t} \left[\mathbf{R}(\alpha_I t)\right] \begin{Bmatrix} u_0 \\ v_0 \end{Bmatrix} \tag{33}$$

with $\left[\mathbf{R}(\alpha_I t)\right]$ being a rotation matrix. A useful fact is that the complex eigen values α_R and α_I of a SDOF complex stiffness system can be determined from the trajectory of $u(t)$ and $v(t)$. Fig. 4(a) represents the time variation of the trajectory radius $r(t)$ which is calculated by

$$r(t) = \sqrt{u^2(t) + v^2(t)} = \mathrm{e}^{-\alpha_R t} \sqrt{u_0^2 + v_0^2} \tag{34}$$

Thus, the real eign value α_R can be determined from the relation given by

$$\ln(r) = -\alpha_R t + \ln\left(u_0^2 + v_0^2\right)/2 \tag{35}$$

between the real eigen value α_R and the trajectory radius r. Meanwhile, Fig. 4(b) represents the time variation of the trajectory phase in radian with respect to the u-axis. Since the trajectory angle is expressed by

$$\tan^{-1}\left(\frac{v(t)}{u(t)}\right) = \alpha_I t + \tan^{-1}\left(\frac{v_0}{u_0}\right) \tag{36}$$

the imaginary eigen value α_I can be determined from the time variation of trajectory angle. One can confirm that the slopes of two plots in Figs. 4 are consistent with the two values $\alpha_R = 4.075$ and $\alpha_I = 50.123$ which are analytically calculated using the formulae given below Eq. (18). Here, the trajectory phase indicates the accumulated value from $t = 0$, and its accumulated value up to $t = 2.0\,sec$ corresponds to about 12 cycles of $u(t)$ and $v(t)$, as can be justified from Fig. 2(a).

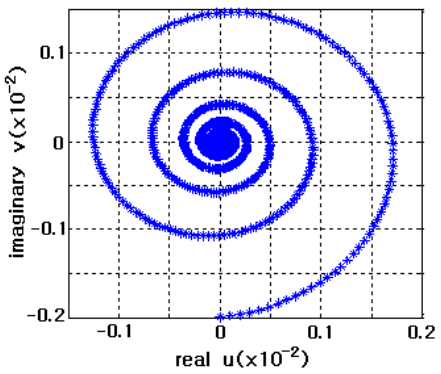

Fig. 3 Trajectory of the real and imaginary parts on the complex plane

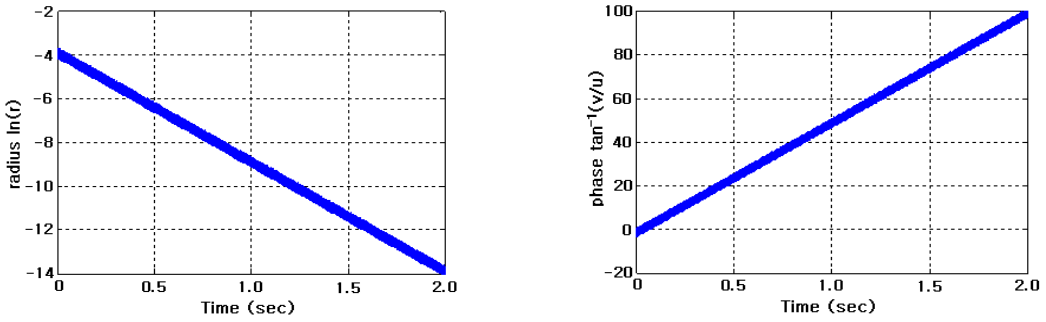

(a) (b)

Fig. 4 Time histories: (a) the trajectory radius and (b) the trajectory phase (*rad*)

Next, the damped forced time response $u(t)$ of the problem (32) to a triangular force having the peak value of $5.0N$ and the duration of $0.5\,sec$ is considered in order to compare the above-mentioned three numerical convolution integration methods and to select the suitable time step size. The convolution integrals in Eqs. (28) and (30) are directly solved by MATHEMATICA to derive the analytically integrated functions of Δt. The damped time responses obtained using the time interval $\Delta t = 0.25\,sec$ are comparatively represented in Fig. 5(a). Except for the first-order approximation method, the other two methods lead to quite inaccurate responses. The superposition method provides almost the vanishing transient response while the zero-order approximation method shows the smaller transient response having a significant time delay. The transient responses of two methods are observed to be improved when the time interval is reduced to $0.05\,sec$ as represented in Fig. 5(b), but still both methods lead to the unacceptable time responses with the inaccurate amplitudes and the time delay. But, the inaccuracy in the amplitude and time delay of two methods disappears when the time interval is further reduced to $0.02\,sec$ as shown in Fig. 5(c), where all three methods provide the time responses which are in excellent agreement with the exact solution. Thus, it has been confirmed that the first-order approximation method provides the time response quite better than the other two methods which exhibit the remarkably inaccurate time integration unless the time interval is sufficiently small. For the current study, the first-order approximation method is used for the next transient response analyses.

We next investigate the correlation between the real and imaginary parts of transient response and compare $v(t)$ and $\mathrm{H}[u(t)]$. Here, $v(t)$ denotes the solution obtained by the present convolution integral (26) while $\mathrm{H}[u(t)]$ indicates the Hilbert transform of $u(t)$. It is not hard to obtain the correlation between the real and imaginary parts of the free response given by

$$\begin{Bmatrix} v(t) \\ \dot{v}(t) \end{Bmatrix} = \alpha_I^{-1} \begin{bmatrix} -\alpha_R & -1 \\ s & \alpha_R \end{bmatrix} \begin{Bmatrix} u(t) \\ \dot{u}(t) \end{Bmatrix} \tag{37}$$

using Eqs. (24) and (25), together with the relation of $s = \alpha_R^2 + \alpha_I^2$. In other words, $v(t)$ and $\dot{v}(t)$ can be obtained from $u(t)$ and $\dot{u}(t)$ using the linear transformation matrix, and vice versa. As well, one can also have the linear correlation given by

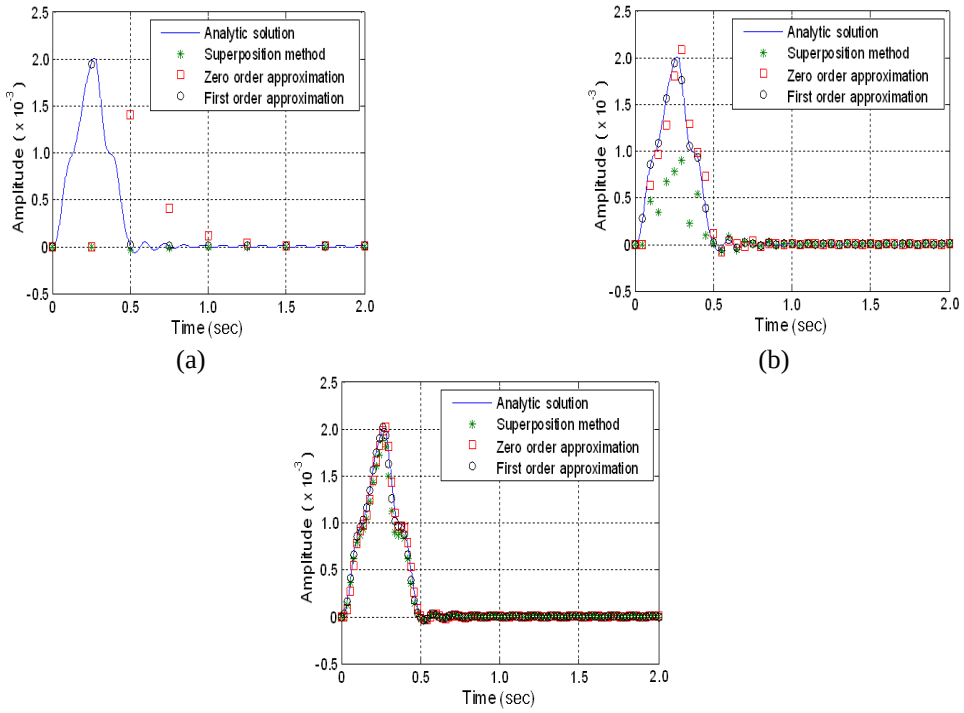

Fig. 5 Transient responses to a triangular force (Bae *et al.* 2014c): (a) $\Delta t = 0.25\,sec$, (b) $\Delta t = 0.05\,sec$ and (c) $\Delta t = 0.02\,sec$

$$\int_0^t f(\tau)\begin{Bmatrix} v(t-\tau) \\ \dot{v}(t-\tau) \end{Bmatrix} d\tau = \alpha_I^{-1}\begin{bmatrix} -\alpha_R & -1 \\ s & \alpha_R \end{bmatrix}\int_0^t f(\tau)\begin{Bmatrix} u(t-\tau) \\ \dot{u}(t-\tau) \end{Bmatrix} d\tau \tag{38}$$

between the real and imaginary parts of the transient response, which can be clearly justified from Figs. 6(a) and 6(b).

Figs. 7(a) and 7(b) represent the complex forced responses to the triangular forces with the peak value of $5.0N$ and the durations of $0.5\,sec$ and $0.01\,sec$ respectively, where $u(t)$ and $v(t)$ are obtained directly by the first-order convolution integral (31). It is observed that $v(t)$ is significantly different from $\mathrm{H}[u(t)]$ for $0.5\,sec$, but this difference completely disappears when the duration of triangular force is reduced from $0.5\,sec$ to $0.01\,sec$. The difference between two complex responses is that Fig. 7(a) is dominated by the forced vibration while Fig. 7(b) is by the free vibration. This comparison implies that the imaginary part $v(t)$ becomes the Hilbert transform of the real part $u(t)$ only when the transient response is not dominated by the forced vibration but by the free response. The physical meaning of the imaginary part $v(t)$ obtained by the present convolution integral will be discussed below in detail.

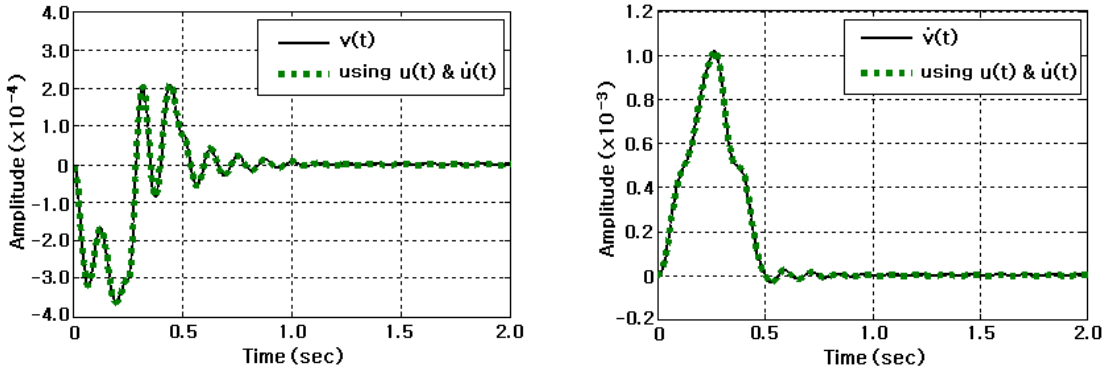

(a) (b)

Fig. 6 Correlation between the real and imaginary parts: (a) displacement $v(t)$ and (b) velocity $\dot{v}(t)$

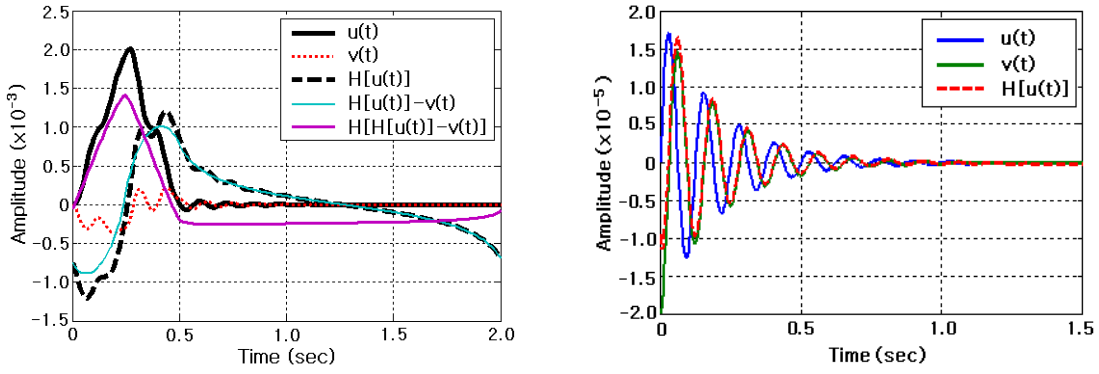

(a) (b)

Fig. 7 Comparison between $v(t)$ and $\mathrm{H}[u(t)]$: (a) at the forced vibration and (b) at the free vibration

As represented in Fig. 7(a), $\mathrm{H}[u(t)]$ contains the oscillation component but $\mathrm{H}[u(t)]-v(t)$ shows a smooth response without the oscillation component. Thus, it is found that $v(t)$ corresponds to the oscillation component which is contained in the Hilbert transform $\mathrm{H}[u(t)]$. It can be also confirmed from the comparison between $\mathrm{H}[\mathrm{H}[\mathrm{H}(u(t))]-v(t)]$ and $u(t)$ that the oscillation component contained in $u(t)$ is not contained in $\mathrm{H}[\mathrm{H}[\mathrm{H}(u(t))]-v(t)]$. Due to this feature, $v(t)$ becomes consistent with the Hilbert transform of $u(t)$ only for the free vibration response, as illustrated in Fig. 7(b). One can analytically justify this fact by examining the correlation between $H[u(t)]$ and $v(t)$ of the following general transient response given by

$$u(t)=\int_0^t F(\tau)e^{-a(t-\tau)}\sin\omega(t-\tau)d\tau+u_0\cos(\omega t)-v_0\sin(\omega t) \tag{39}$$

$$v(t)=\int_0^t F(\tau)e^{-a(t-\tau)}\cos\omega(t-\tau)d\tau+u_0\sin(\omega t)+v_0\cos(\omega t) \tag{40}$$

of the SDOF forced vibration problem in Eq. (11). The last two terms on RHS in each equation correspond to the free response, and those are clear in the relation of Hilbert transform. On the other hand, the transient response by the first integral form on RHS in both equations violates the relation of Hilbert transform, which can be justified by letting $F(\tau)=c_0+c_1\tau+c_2\tau^2+\cdots$, by integrating term by term, and by comparing the Hilbert transforms of integrated terms in $u(t)$ with their counter parts in $v(t)$. One can find out that the harmonic oscillation parts in $v(t)$ and $H[u(t)]$ are identical but the remaining parts are different.

Next, we investigate whether the direct mathematical differentiation of transient displacements $u(t)$ and $v(t)$ coincide with the transient velocities $\dot{u}(t)$ and $\dot{v}(t)$ or not. In case of the real part, du/dt is exactly the same with $\dot{u}(t)$ as represented in Fig. 8(a). But, it is observed from Fig. 8(b) that this exact correlation does not hold any more for the imaginary part. That is

$$\frac{d}{dt}\int_0^t f(\tau)v(t-\tau)d\tau\neq\int_0^t f(\tau)\dot{v}(t-\tau)d\tau \tag{41}$$

It can be proved by substituting the free responses $v(t)=-\mathrm{e}^{-\alpha_R t}\cos(\alpha_I t)/\alpha_I$, $\dot{v}(t)=\mathrm{e}^{-\alpha_R t}[\sin(\alpha_I t)+\alpha_R\cos(\alpha_I t)/\alpha_I]$ into Eq. (41) for arbitrary external force $f(t)$ (for example, a constant force). In Eq. (41), the left formula does not leave integration constant differing from the right formula, so the difference may occur whenever the integration constant appears.

Next, we applied a harmonic force $f(t)=a\sin(\omega t)$ with $a=5.0N$ and $3.0Hz$ to the problem (32), in order to examine once again the correlation between $u(t)$ and $v(t)$ and the other useful relations. Fig. 9(a) compares the transient responses that were obtained by three different numerical integration methods using the time interval Δt of $0.02\,sec$.

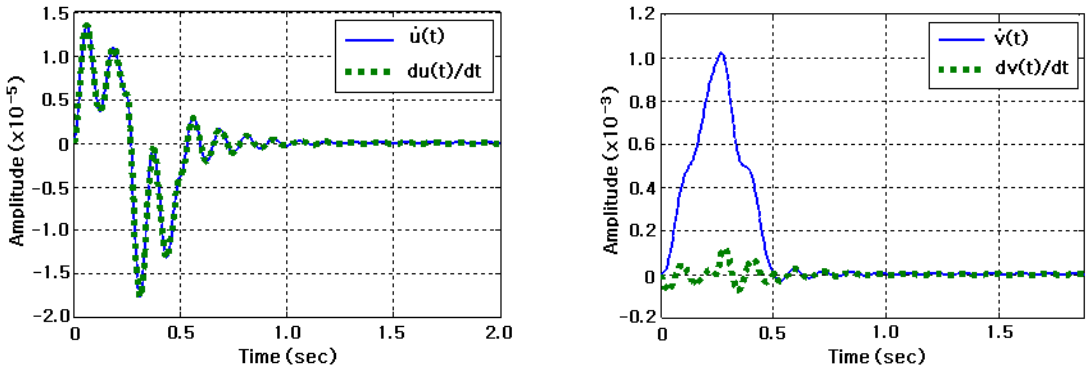

(a) (b)

Fig. 8 Comparison at the level of velocity: (a) real part $\dot{u}(t)$ and (b) imaginary part $\dot{v}(t)$

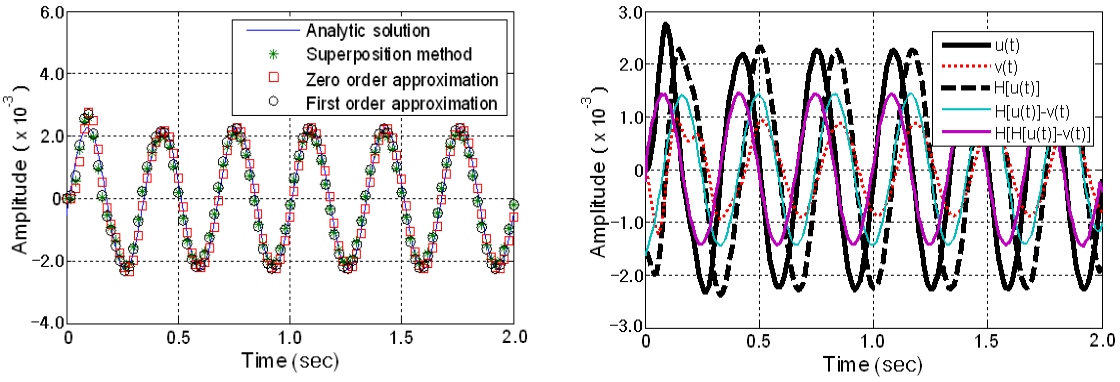

(a) (b)

Fig. 9 (a) Transient responses to a harmonic force ($\Delta t = 0.02\,sec$) and (b) relation between the real and imaginary parts

As in the previous case for the triangular impulse force, all three methods provide the forced transient responses that are in excellent agreement with the analytic solution, except for a slight difference at the first peak. We use the numerical solution obtained by the first-order approximation method for further investigation. Fig. 9(b) comparatively represents the real and imaginary parts, the Hilbert transform $H[u(t)]$ and the differences between them. First of all, the phase difference $\pi/2$ but the equal amplitude between $u(t)$ and $H[u(t)]$ are clearly observed, except at the beginning. This correlation is also observed from $H[u(t)]-v(t)$ and its Hilbert transform $H[H[u(t)]-v(t)]$. Regarding the relation between $H[u(t)]$ and $v(t)$, it is clear that both exhibit the same harmonic oscillation response with the same phase angle, except at the beginning, which confirms that $v(t)$ becomes the oscillation component contained in $\mathrm{H}[u(t)]$. Meanwhile, both shows the remarkable difference in their amplitudes, which is because $u(t)$ in this case is not free response but forced one, differing from Fig. 7(b).

We next examine the relation in Eq. (38) for alternatively obtaining $v(t)$ and $\dot{v}(t)$ from $u(t)$ and $\dot{u}(t)$. It is clear from Fig. 10 that the relation (38) provides the responses that are exactly same with $v(t)$ and $\dot{v}(t)$. Next, we examine whether the direct mathematical differentiation of transient displacements $u(t)$ and $v(t)$ coincide with the transient velocities $\dot{u}(t)$ and $\dot{v}(t)$ or not. As represented in Fig. 11, it is found that du/dt is exactly the same with $\dot{u}(t)$ but dv/dt is totally different from $\dot{v}(t)$. Thus, it has been confirmed that both relations also hold for the forced transient response by the harmonic force, as in the previous case for the triangular impulse force.

The above-mentioned characteristics of the transient response $\mathbf{x}_a(t) = \{u(t), \dot{u}(t), v(t), \dot{v}(t)\}^T$ of a SDOF complex stiffness system which is obtained by the convolution integral (26) are summarized in the diagram shown in Fig. 12.

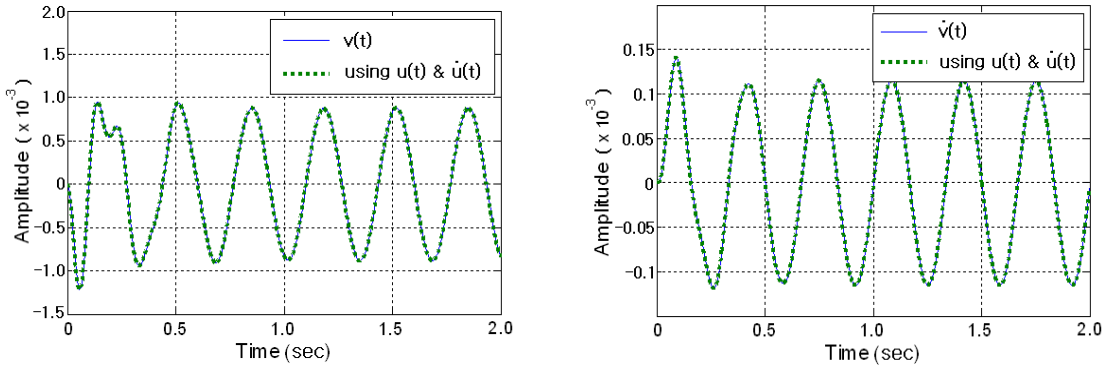

(a) (b)

Fig. 10 Correlation between the real and imaginary parts: (a) displacement $v(t)$ and (b) velocity $\dot{v}(t)$

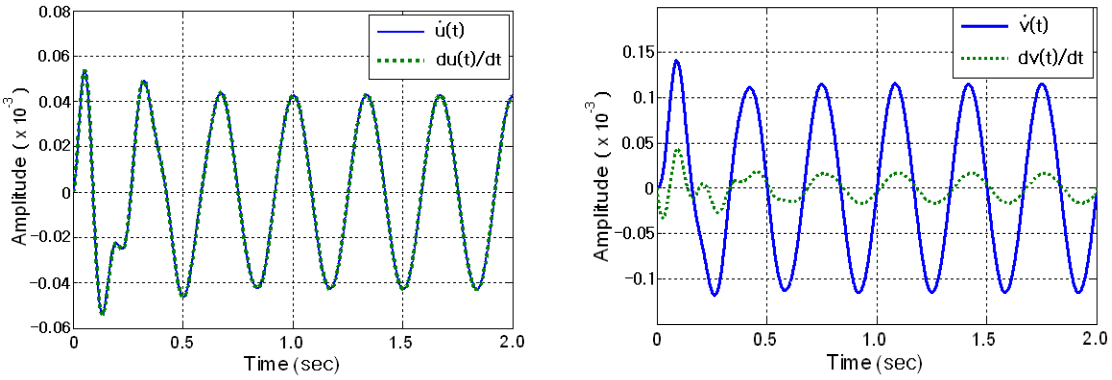

(a) (b)

Fig. 11 Comparison at the level of velocity: (a) real part $\dot{u}(t)$ and (b) imaginary part $\dot{v}(t)$

First of all, the real and imaginary parts are in the correlation via a linear matrix of complex eigen values, such that one part can be obtained from the counter part using this linear correlation. But, the imaginary part $v(t)$ is identical only with the oscillation component contained in the Hilbert transform $\mathrm{H}[u(t)]$ of the real part, and vice versa, so that the correlation with the Hilbert transform holds only when the transient response is dominated by the harmonic response. Meanwhile, the direct mathematical differentiation does hold only for the real part $u(t)$ of the complex transient response

Thus, these characteristics explained above could help one to model and simulate the free and transient responses of linear complex system using Simulink and MATHEMATICA. The relation between the real and imaginary parts could be implemented by Simulink while the numerical integration could be obtained by MATHEMATICA.

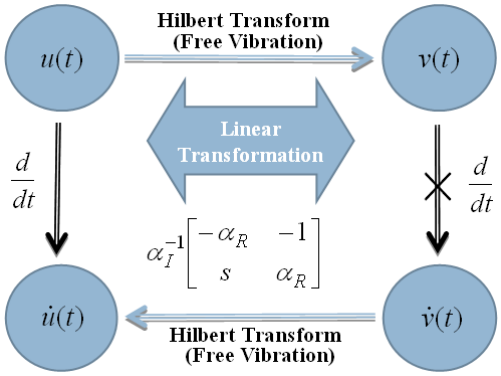

Fig. 12 Diagram showing the correlation between the real and imaginary parts

6. Conclusions

In this paper, a numerical convolution integral by utilizing the Hilbert transform for obtaining the transient response of SDOF complex stiffness system was introduced, and the characteristics of transient response obtained by the proposed method were investigated. By assuming the imaginary part to be the Hilbert transform of the real part, the analytic solution was expressed by a sum of real and imaginary parts. The free response of SDOF complex stiffness system and the consistent imaginary initial conditions were derived in the state-space formulation. And, the transient response was obtained by the numerical convolution integration of the discrete impulse forces and the unit impulse response.

Through the preliminary numerical experiments, it was justified that the solution is expressed by a product of time-exponential and time-harmonic functions and the imaginary part exhibits the phase delay of $\pi/2$. It was also observed that the real and imaginary eigen values of the complex system can be determined from the time variations of the radius and phase of the trajectory of $u(t)$ and $v(t)$ on the complex plane. Meanwhile, from the comparative experiments of three numerical convolution integral methods, it was found that the first-order approximation method provides the numerical accuracy much better than the other two methods.

From the characteristic investigation of the transient responses, it was found that the real and imaginary parts are in correlation via a linear matrix of complex eigen values, so that either part can be obtained from its counter part using this linear correlation. But, the imaginary part of transient response coincides with the Hilbert transform of the real part only when the response is not dominated by the forced vibration, because it corresponds to the oscillation contained in the Hilbert transform. Furthermore, the direct mathematical differentiation of the imaginary transient response does not coincide with the convolution integral of free response $\dot{v}(t)$, because it does not leave the integration constant, differing from the convolution integral.

Meanwhile, the cases in which the forced vibration is dominated would be worthwhile, and the development of accurate time-domain analysis method for such cases, together with its characteristic investigation, represents a topic that deserves future work.

Acknowledgements

This study was financially supported by the 『2016 Post-Doc. Development Program』 of Pusan National University.

References

Bae, S.H., Cho, J.R. and Jeong, W.B. (2014a), "A discrete convolutional Hilbert transform with the consistent imaginary initial conditions for the time-domain analysis of five-layered viscoelastic sandwich beam", *Comput. Method. Appl. M.*, **268**, 245-263.

Bae, S.H., Cho, J.R. and Jeong, W.B. (2014b), "Time-duration extended Hilbert transform superposition for the reliable impact response analysis of five-layered damped sandwich beams", *Finite Elem. Anal. Des.*, **90**, 41-49.

Bae, S.H., Jeong, W.B. and Cho, J.R. (2014c), "Transient response of complex stiffness system using a green function from the Hilbert transform and the steady space technic", *Proc. Inter.noise*, 1-10.

Chen, L.Y., Chen, J.T., Chen, C.H. and Hong, H.K. (1994), "Free vibrations of a SDOF system with hysteretic damping", *Mech. Res. Commun.*, **21**, 599-604.

Chen, J.T. and You, D.W. (1997), "Hysteretic damping revisited", *Adv. Eng. Softw.*, **28**, 165-171.

Cho, J.R., Lee, H.W., Jeong, W.B., Jeong, K.M. and Kim, K.W. (2013), "Numerical estimation of rolling resistance and temperature distribution of 3-D periodic patterned tire", *Int. J. Solids Struct.*, **50**, 86-96.

Crandall, S.H. (1995), "A new hysteretic damping model?", *Mech. Res. Commun.*, **22**, 201-202.

Fink, M. (1992), "Time reversal of ultrasonic fields, I. Basic principles", *IEEE T. Ultrason. Ferr.*, **39**(5), 555-566.

Genta, G. and Amati, N. (2010), "Hysteretic damping in rotordynamics: An equivalent formulation", *J. Sound Vib.*, **329**(22), 4772-4784.

Hajianmaleki, M. and Qatu, M.S. (2013), "Vibrations of straight and curved composite beams: A review", *Comput. Struct.*, **100**, 218-232.

Inaudi, J. and Makris, N. (1996), "Time-domain analysis of linear hysteretic damping", *Earthq. Eng. Struct. D.*, **25**, 529-545.

Johansson, M. (1999), *The Hilbert Transform*, Master Thesis, Växjö University.

Li, Z., Qiao, G., Sun, Z., Zhao, H. and Guo, R. (2012), "Short baseline positioning with an improved time reversal technique in a multi-path channel", *J. Marine Sci. Appl.*, **11**(2), 251-257.

Luo, H., Fang, X. and Ertas, B. (2009), "Hilbert transform and its engineering applications", *AIAA J.*, **47**(4), 923-932.

Mead, D.J. and Markus, S. (1969), "The forced vibrations of a three-layer, damped sandwich beam with arbitrary boundary conditions", *J. Sound Vib.*, **10**(2), 163-175.

Meirovitch, M. (1986), *Elements of Vibration Analysis*, McGraw-Hill.

Mohammadi, F. and Sedaghati, R. (2012), "Linear and nonlinear vibration analysis of sandwich cylindrical shell with constrained viscoelastic core layer", *Int. J. Mech. Sci.*, **54**(1), 156-171.

Nguyen, H., Andersen, T. and Pedersen, G.F. (2005), "The potential use of time reversal techniques in multiple element antenna systems", *IEEE Commun. Lett.*, **9**(1), 40-42.

Rao, S.S. (1995), *Mechanical Vibrations*, 3rd eds, Singapore.

Padois, T., Prax, C., Valeau, V. and Marx, D. (2012), "Experimental localization of an acoustic sound source in a wind-tunnel flow by using a numerical time-reversal technique", *Acoust. Soc. Am.*, **132**(4), 2397.

Sainsbury, M.G. and Masti, R.S. (2007), "Vibration damping of cylindrical shells using strain-energy-based distribution of an add-on viscoelastic treatment", *Finite Elem. Anal. Des.*, **43**, 175-192.

Salehi, M., Bakhtiari-Nejad, F. and Besharati, A. (2008), "Time-domain analysis of sandwich shells with passive constrained viscoelastic layers", *Scientia Iranica*, **15**(5), 637-43.

Wang, Z.C., Geng, D., Ren, W.X., Chen, G.D. and Zhang, G.F. (2015), "Damage detection of nonlinear

structures with analytical mode decomposition and Hilbert transform", *Smart Struct. Syst.*, **15**(1), 1-13.
Won, S.G., Bae, S.H., Cho, J.R., Bae, S.R. and Jeong, W.B. (2013), "Three-layered damped beam element for forced vibration analysis of symmetric sandwich structures with a viscoelastic core", *Finite Elem. Anal. Des*., **68**, 39-51.
Zhu, H., Hu, Y. and Pi, Y. (2014), "Transverse hysteretic damping characteristics of a serpentine belt: Modeling and experimental investigation", *J. Sound Vib*., **333**(25), 7019-7035.

CC